Int. J. Heat Mass Transfer. Vol. 26, No. 2, pp. 197–209, 1983
Printed in Great Britain

0017-9310/83/020197-13 $03.00/0
Pergamon Press Ltd.

GAS TURBINE COMBUSTOR MODELLING FOR CALCULATING POLLUTANT EMISSION

G. ROMBERG
DFVLR, Institut für Theoretische Strömungsmechanik, Göttingen, Federal Republic of Germany

(*Received* 5 *February* 1982)

Abstract—In this paper two aspects of can and annular combustor primary zone flows are considered in detail. Firstly, pollutant production and transport in the primary zone are described by a 3-dim. mathematical model. Secondly, the mechanical and thermodynamic state of the flow at the primary zone exit is described by a 1-dim. mathematical model. The general system function of a connection in series of the two models provides the NO emission from the primary zone in terms of engine operating parameters such as fuel injection rate and water injection rate. The modelling method shows an important effect of the ratio of the cooling air inflow to the combustion air inflow on NO emission. Also, the influence of dissociation on the flow at the primary zone exit is analyzed.

NOMENCLATURE

A, total inflow of air into the primary zone;
B, combustion air inflow into the primary zone;
c_i, mass fraction of species i;
c_p, specific heat at constant pressure of the exhaust gas;
c_{pi}, specific heat at constant pressure of species i;
c_{N_2}, mass fraction of N_2, equation (23);
e_i, emission rate of pollutant i from the primary zone;
E, area of $\mathscr{F}$;
F, fuel injection rate;
g, N_2/air ratio, equation (4);
h_i, enthalpy of species i;
i_ω, outflow of species i, equation (3);
K_r, equilibrium constant of the rth reaction;
M, Mach number;
$M_{i\omega}(t)$, total amount of pollutant i, defined by equation (13);
n, number of species;
p, pressure;
$\overline{P_\omega}$, probability density, equation (12);
t, time;
T, temperature;
v, flow velocity;
W, molecular weight of the exhaust gas;
W_i, molecular weight of species i;
W_f, molecular weight of the fuel;
$\mathbf{x}$, position vector.

Greek symbols

ρ, density;
$\overline{\rho_{i\omega}}$, average density, equation (12);
Φ, fuel/O_2 ratio;
φ, equivalence ratio, equation (42);
Ψ, H_2O/O_2 ratio;
ψ, H_2O/dry air ratio;
ε, N_2/O_2 ratio;
Ω, number of surface elements of $\mathscr{P}$;
$\nu'_{ir}, \nu''_{ir}, \nu'_f$, stoichiometric coefficients, equations (6) and (42);
γ, O_2/air ratio;
γ_d, O_2/dry air ratio;
κ, ratio of specific heats;
χ, Ar/N_2 ratio.

Other symbols

$\mathscr{P}$, part of the inner zone surface;
$\mathscr{F}$, primary zone exit (i.e. a cross section).

Subscripts

t, reservoir conditions;
e, unconstrained equilibrium;
E, primary zone exit;
ω, surface element of $\mathscr{P}$;
$(\,)_0$, composition at low temperature where dissociation is negligible.

Superscripts

$\hat{}$, particular composition, equations (28) and (29);
$\bar{}$, ensemble average.

INTRODUCTION

FIGURE 1 shows the mean flow pattern in a typical combustor (flame tube). It can be divided roughly into two parts, a primary and a secondary zone. In the primary zone, one fraction of the air enters the combustor through swirlers around the fuel spray nozzle. In the walls of the combustor body are a selected number of holes through which a further fraction passes into the primary zone. The air from the swirl vanes interacts with that from the primary air holes and creates a region of low velocity recirculation. This takes the form of a toroidal vortex, and has the effect of stabilizing and anchoring the combustion process. The remainder of the primary air enters the primary zone through slots and is used to film-cool the walls of the combustor. Different divisions of a gas turbine combustor into zones have been proposed. Some

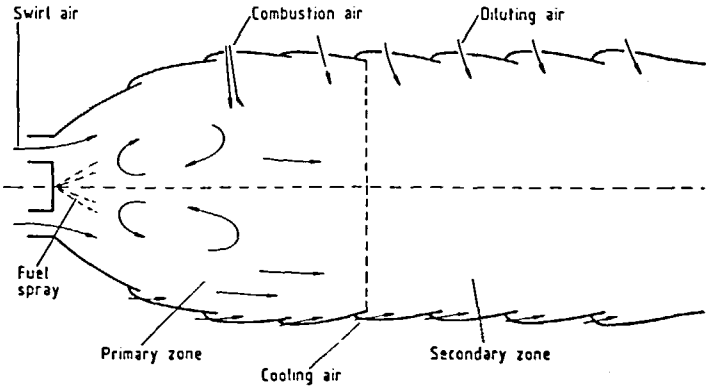

FIG. 1. Cross section of a typical combustor liner: upper half shows flow through combustion air and diluting air holes; lower half shows film-cooling air.

authors distinguish three zones [1]: a primary zone in which fuel is injected into a recirculating airstream and where most of the burning takes place, followed by an intermediate zone in which combustion proceeds to completion. Downstream of this zone is a dilution zone where further air is injected to cool the gas down to the turbine inlet temperature. The term secondary zone as used by other authors [2] comprises the intermediate and secondary zone outlined above. Some authors denote the upstream part of the combustor in which the total burning takes place as primary zone followed by a secondary zone where further air is injected to cool the gas down to the turbine inlet temperature [3].

There are three main types of conventional combustion chambers at present in use for gas turbine aeroengines. These are the multiple chamber, the annular chamber and the tubo-annular chamber.

Multiple combustion chamber. The chambers are disposed around the engine and compressor delivery air is directed by ducts to pass into the individual chambers. Each chamber has an inner flame tube (can combustor) around which there is an air casing. The air passes through the flame tube and also between the tube and the outer air casing.

Annular combustion chamber. The flame tube in this instance forms an annulus around the engine, open at one end to the compressor and at the other end to the turbine nozzles. An inner and outer air casing contains the flame tube. Holes in the flame tube allow air to enter the tube from the annular space between the tube and the inner air casing and also from the annular space between the tube and the outer air casing.

Tubo-annular combustion chamber. This type is a combination of the previous types. A number of flame tubes (can combustors) are fitted inside a common air casing.

Figure 1 applies to a can combustor of conventional tubo-annular or of multiple combustion chambers and to conventional annular chambers.

In early work on combustor modelling for calculating pollutant emission, the primary zone flow is represented either as a plug flow or as a well-stirred reactor [2]. In the latter model, gases flow steadily through and react within the reaction vessel. Turbulent mixing is assumed to be much more rapid than chemical reaction and sufficiently intense to maintain the time-averages of the following quantities constant throughout the reaction vessel of volume V: temperature T, pressure p, partial densities ρ_i, mass fractions c_i of all species and the mass production rate of species i per unit volume in the rth reaction, Γ_{ir}. Therefore, if all parts of the gas flow are assumed to remain in the reaction vessel for a time equal to the mean residence time

$$\tau_R = \frac{\bar{\rho} V}{\dot{m}}$$

where $\dot{m}$ and ρ are, respectively, the mass flow rate through the vessel and the mass density, and the overbar denotes a time-average, then the change in mass fraction of species i on passing through the vessel is simply

$$\bar{\rho}(\overline{c_{i1}} - \overline{c_{i0}}) = \tau_R \sum_{r=1}^{R} \overline{\Gamma_{ir}}.$$

The quantities $\overline{c_{i0}}$ and $\overline{c_{i1}}$ are the mass fractions of the incoming and outgoing stream, respectively. Conventionally, the effects of fluctuations on $\overline{\Gamma_{ir}}$ are ignored and it is evaluated from the expression for Γ_{ir} with $T = \bar{T}$, $\rho = \bar{\rho}$ and $c_j = \overline{c_j}$ $(j = 1, \ldots, n)$, where n is the number of species. (R is the number of reactions.)

The pollutant emission from the primary zone depends on chemical reactions and on fluid mechanical processes, which involve the mixing of the various species. The simple-reactor model briefly outlined before can describe the influence of reaction kinetics. However, it cannot take sufficient account of the fluid mechanical processes.

Two concepts have been proposed to overcome this shortcoming:

(1) The primary zone is treated as a statistical series of well-stirred reactors, with a distribution of equivalence ratios and a distribution of residence times [4]. The determination of these distributions relies on experiments on an appropriate physical model.

(2) The primary zone is treated as an arrangement of well-stirred reactors. The influence of fluid mechanical processes on pollutant production is built into this system using information from a 'flow field model' [5, 6].

In the former approach the difficult problem of constructing a physical model with a known similarity between prototype and laboratory model must be fixed. The latter approach entails the solution of an extremely difficult closure problem associated with a non-isotropic turbulence model (ref. [7], p. 90) and a tremendous amount of numerical work. Furthermore, the method of combining the flow field model with an arrangement of well-stirred reactors is not straightforward, perhaps because an arrangement of well-stirred reactors is too rigid to have the fluid mechanical processes built into it in an appropriate way.

The two modelling concepts have in common the gross structure illustrated in Fig. 2. Broken and solid lines indicate input and output, respectively. Unspecified system properties of an arrangement of well-stirred reactors A are specified by output information from element B. In concept 2 element B is a mathematical model (flow field model). In concept 1 element B comprises a suitable physical model (model combustor) and a mathematical model connected in series. The system function of the mathematical part is a similarity relation between the model combustor and the prototype.

The mathematical model for calculating pollutant emission from the primary zone presented in this paper is tailored to take appropriate account of both fluid mechanical processes and chemical processes. This model utilizes modern trends in combustor design (e.g. increase of combustor inlet air pressure and temperature). The use of the present model requires a comparatively small amount of numerical work which is in reasonable proportion to the attainable output.

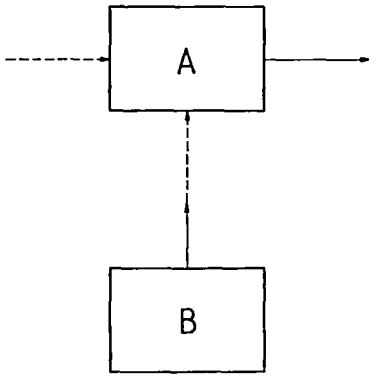

FIG. 2. Gross structure of the two modelling concepts.

Also, the present modelling method provides the flow velocity and the thermodynamic quantities at the primary zone exit which constitute the starting base for the secondary zone modelling envisaged.

MODELLING CONCEPTS

General experience as a guide to model design

The conventional combustor can be divided into two parts, a primary and a secondary zone. Within the primary zone the total burning takes place. Embedded in this zone is a region of low velocity recirculation which has the effect of stabilizing the combustion process. In the secondary zone dilution air is mixed with the gas stream from the primary zone to cool it to the temperature required at the turbine inlet. A combustor has various devices for metering the distribution of the total airflow along the chamber. This distribution is illustrated in Fig. 1. One fraction of the total airflow is used in the primary zone for combustion and wall cooling. It enters the primary zone through swirlers and holes, and slots, respectively, in the combustor wall. The remaining fraction is introduced progressively into the secondary zone through holes and slots in the combustor wall. The foregoing brief account of combustors applies to most types over a wide operating range, although the design of a combustor and the method of adding the fuel may vary considerably. These generalizations are substantiated by extensive experience pertinent to gas turbine combustor modelling.

Turbulent combustion in gas turbine combustors is far from being fully understood [7–9] and a breakthrough towards a satisfactory clarification does not seem to be in sight. It is a noteworthy feature of the literature pertinent to turbulent combustion that many authors, making assumptions which contradict assumptions made by others, still find experimental evidence in support of their hypotheses. This is presumably partly because turbulent combustion is a most complex phenomenon having many possible structures. More important, in the opinion of several authors [8, 9], is the lack of comprehensive and accurate experimental data with which to test the various hypotheses. The structures of turbulent combustion which have been reported in liquid-fueled conventional combustors can be grouped into two categories:

(1) Combustion localized in the narrow sheet of a flame.

(2) Combustion distributed over a volume.

In the former category the flame front is located at the periphery of the spray sheath and the combustion of the spray is similar to that of a gaseous turbulent diffusion flame (ref. [10], p. 27-20 and ref. [7], p. 192). The latter category comprises the model of laminar diffusion flames around individual droplets (ref. [11], p. 52) and the model of burning turbulent eddies (ref. [12], p. 21-3). In this model the fuel droplets vaporize, then fuel vapour and air mix to form turbulent eddies of

combustible mixture. As each eddy ignites, either a thin flame front will propagate through the eddy or envelop and consume the eddy, depending on the local fuel–air ratio and the eddy size.

General modelling philosophy

It is evident from the foregoing brief state-of-the-art report that a comprehensive quantitative description of the liquid-fueled primary zone of a conventional gas turbine combustor is beyond reach. But a mathematical model is feasible whose system function provides partial information (say the pollutant emission from the primary zone exit (output)) in terms of engine-operating parameters relevant to pollutant emission from the primary zone exit (input). This is because this type of model requires much less information about the complex processes in the primary zone than a comprehensive quantitative description.

Gross structure of the present model

The mathematical model A is tailored to account for the influence of the fluid mechanical processes on the pollutant emission from the primary zone. Built into A is a thermodynamic system whose unspecified properties concerning chemical conversion are specified by output information from the chemical model C. The chemical model is essentially a chemical reaction mechanism which may be approximate or exact.

Design of the fluid mechanical model

The design is based on the general experience described at the beginning of this section and must be in accord with this experience.

Consider a conventional liquid-fueled combustor in a steady operating state. Steady state means all probability densities pertinent to the primary zone flow are independent of time t or time origin. The primary zone can be divided into an outer zone whose outer surface coincides with the primary zone surface, and Λ separate inner zones z_λ ($\lambda = 1,\ldots,\Lambda \geqslant 1$) which are surrounded by the outer zone and where most of the burning takes place.

The pollutants at the primary zone exit are pollutants contained in elements of burnt fluid. Each of these elements originates from an inner zone, passes through the surface of this zone and then moves towards the primary zone exit within the outer zone while retaining its identity. (Therefore molecular diffusion across the surface of the fluid element is negligible.) When such an element of burnt fluid is leaving the inner zone from which it originates, the combustion in it may be complete or incomplete* at a fuel to molecular oxygen (O_2) ratio Φ between fuel-rich and fuel-lean, at a water vapour to O_2 ratio Ψ and at a molecular nitrogen (N_2) to O_2 ratio ε. The ratios ε and Ψ may deviate from the corresponding values of the air at the primary zone inlet. The uncertainty in Φ, ε and Ψ is strongly influenced by the action of turbulence and molecular diffusion.

We assume that the elements of burnt fluid under consideration exhibit unconstrained thermodynamic equilibrium at pressure $p = p_E$ and temperature $T = T_E$ when they pass across the primary zone exit. p_E and T_E are an average pressure and an average temperature at the primary zone exit, respectively. Laboratory experiments (ref. [11], p. 62) and estimates [2] based on primary zone conditions, typical for engine designs which were widely used in the early 1970s, indicate that the NO mass fraction at the primary zone exit deviates from its equilibrium value at local pressure, temperature and equivalence ratio. This deviation proves to be very temperature sensitive, so that it will become negligible when any design change leads to a relatively small increase of the flame temperature in the primary zone. In modern engine technology the trend is towards higher combustor inlet air temperature and pressure so that the above assumption will be appropriate for future advanced engines over a wide range of operating states (e.g. ref. [12], p. 21-15) at least for the purpose of calculating the NO emission from the primary zone.

We denote by A, B, C and C_E the ensemble averages of the following quantities: total inflow of air into the primary zone; combustion air inflow into the primary zone; cooling air inflow into the primary zone and the outflow of air, not involved in combustion, across the primary zone exit (i.e. the interface between primary and secondary zone). The following balance equations then apply

$$C + B = A \tag{1}$$

and

$$C = C_E. \tag{2}$$

Let i_ω be the ensemble-averaged outflow of species i in the above described elements of burnt fluid on passing across the surface element ω of the inner zone. We then have, in the absence of chemical conversion within the elements of burnt fluid,

$$i_\omega = (i_\omega)_E \tag{3}$$

where $(i_\omega)_E$ is the ensemble-averaged outflow of species i in the elements burnt fluid on passing across the primary zone exit on their path downstream from surface element ω. The part $\mathscr{P}$ of the surface of the inner zone where $i_\omega > 0$, is subdivided into Ω elements such that

$$i_\omega = g\frac{B}{\Omega}, \tag{4}$$

where i refers to molecular nitrogen. (g is the molecular nitrogen to air ratio of the air at the primary zone inlet.)

Thermodynamic and chemical model

The thermodynamic model is allocated to the

*The thermodynamic equilibrium in it may be unconstrained or constrained.

elements of burnt fluid described above. It is described by Gibbs' equation

$$ds = \frac{du}{T} + \frac{p}{T} d\left(\frac{1}{\rho}\right) - \sum_{i=1}^{n-1} \frac{\mu_i - \mu_n}{T} dc_i \quad (5)$$

where s is the enthropy per unit mass, u is the internal energy per unit mass and μ_i is the chemical potential of species i. The chemical reactions within the elements of burnt fluid can be written as

$$\sum_{i=1}^{n} \nu'_{ir} S_i \leftrightarrows \sum_{i=1}^{n} \nu''_{ir} S_i, \quad r = 1, \ldots, R \quad (6)$$

where S_i denotes a species i particle and ν'_{ir} and ν''_{ir} denote stoichiometric coefficients for reaction r. Formula (6) formally represents the chemical model.

Let $I < n$ be the maximum number of independent reactions among the R reactions. I mass fractions c_i can then be varied independently. We can number them such that $c_1, \ldots, c_I$ are independent mass fractions. The remaining mass fractions depend linearly on $c_1, \ldots, c_I$

$$dc_i = \sum_{k=1}^{I} \zeta_{ik} \, dc_k, \quad i > I. \quad (7)$$

The coefficients ζ_{ik} are determined by the stoichiometric coefficients of the independent reactions and the molecular weights W_i of the species i ($i = 1, \ldots, n$). Substituting equation (7) into Gibbs' equation gives

$$ds = \frac{du}{T} + \frac{p}{T} d\left(\frac{1}{\rho}\right) + \sum_{i=1}^{I} \frac{A_i}{T} dc_i \quad (8)$$

where

$$A_i = -\left(\mu_i + \sum_{k=I+1}^{n} \zeta_{ki} \mu_k\right) \quad (9)$$

is the affinity of species i.

DETERMINATION OF THE SYSTEM FUNCTION

General formula

Consider a small spherical vicinity $\mathscr{H}$ of a position $\mathbf{x} = \mathbf{x}_E$ at the primary zone exit. x denotes the position vector. The diameter of this vicinity is sufficiently small so that the ensemble-averaged density of pollutant i due to the elements of burnt fluid from the surface element ω, $\overline{\rho_{i\omega}}(\mathbf{x})$, can be considered as independent of position in this vicinity. The characteristic dimensions of the elements of burnt fluid in this vicinity of volume V can be assumed to be very small compared to the diameter of $\mathscr{H}$.

Let N_ω be the number of elements of burnt fluid which leave the inner zone across ω on $\mathscr{P}$ during a small time interval $t_a \leqslant \vartheta \leqslant t_b$. ϑ is a time variable, t_a a lower bound and t_b an upper bound. The number N_ω and the surface $\mathscr{P}$ are considered not to vary in the ensemble of realizations including the prototype over which the ensemble average is taken. Let us define (for the ensemble)

$$P_\omega(\mathbf{x}_E, t, \mathbf{x}_\omega, t_c) = V^{-1} \quad (10)$$

if the marked element of burnt fluid which was at position $\mathbf{x} = \mathbf{x}_\omega$ on ω at times t_c lies in $\mathscr{H}$ at time $t > t_b$, otherwise

$$P_\omega(\mathbf{x}_E, t, \mathbf{x}_\omega, t_c) = 0. \quad (11)$$

We can think of the ensemble mean $\overline{P_\omega(\mathbf{x}_E, t, \mathbf{x}_\omega, t_c)}$ as the probability density of finding, at time t and position $\mathbf{x}_E$, the marked element of burnt fluid which was at position $\mathbf{x}_\omega$ at time t_c. We denote by $m_{i\omega}(t)$ the amount of pollutant i in any of the N_ω fluid elements at time t. Without loss in generality $m_{i\omega}(t)$ can be considered to be equal for all N_ω fluid elements at time t, in this way utilizing the freedom of subdivision of the burnt fluid in the outer zone into elements. $m_{i\omega}(t)$ (but not N_ω) may vary from realization to realization.

The ensemble-averaged density of pollutant i at $\mathbf{x}_E, t$ due to the N_ω elements under consideration can be written as

$$\overline{\rho_{i\omega}}(\mathbf{x}_E, t) = \overline{M_{i\omega}(t) \, P_\omega(\mathbf{x}_E, t, \mathbf{x}_\omega, t_b)}, \quad (12)$$

assuming (first 'closure assumption')

$$\left| \frac{M_{i\omega}(t)}{\overline{M_{i\omega}(t)}} - 1 \right| \ll 1, \quad M_{i\omega}(t) = N_\omega m_{i\omega}(t). \quad (13)$$

$M_{i\omega}(t)$ denotes the total amount of pollutant i in the N_ω fluid elements at time t.

Truncating the Taylor expansion of $\overline{M_{i\omega}(t)}/\overline{M_{i\omega}(t_b)}$ with respect to $t_b - t_a$ after the first term, we obtain

$$\frac{\overline{M_{i\omega}(t)}}{\overline{M_{i\omega}(t_b)}} = Q_{i\omega}(t - t_b). \quad (14)$$

Steady operating state implies that the first term $Q_{i\omega}$, as well as the probability density $\overline{P_\omega}$, cannot depend on t and t_b separately but on the combination $t - t_b$ only,

$$\overline{P_\omega(\mathbf{x}_E, t, \mathbf{x}_\omega, t_b)} = \overline{P_\omega}(\mathbf{x}_E, \mathbf{x}_\omega, t - t_b). \quad (15)$$

Combining equations (12), (14), (15) and

$$\overline{M_{i\omega}(t_b)} = i_\omega (t_b - t_a) \quad (16)$$

gives

$$\overline{\rho_{i\omega}}(\mathbf{x}_E, t) = Q_{i\omega}(t - t_b) \overline{P_\omega}(\mathbf{x}_E, \mathbf{x}_\omega, t - t_b) i_\omega (t_b - t_a). \quad (17)$$

The interval $-\infty \leqslant \vartheta \leqslant t$ is divided into equal sub-intervals. The interval $t_a \leqslant \vartheta \leqslant t_b$ can be considered to be any of these sub-intervals. The ensemble-averaged density of pollutant i at position $\mathbf{x}_E$ due to the elements of burnt fluid from surface element ω, $\overline{\rho_{i\omega}}(\mathbf{x}_E)$, can be represented as a sum of contributions which are of the type of the term on the RHS of equation (17). Hence,

$$\overline{\rho_{i\omega}}(\mathbf{x}_E) = i_\omega \int_0^\infty Q_{i\omega}(\tau) \overline{P_\omega}(\mathbf{x}_E, \mathbf{x}_\omega, \tau) \, d\tau \quad (18)$$

where τ is an integration variable. Denoting by v the axial component (in the downstream direction) of the ensemble-averaged flow velocity, multiplying equation (18) by v, and then integrating over the primary zone

exit $\mathscr{F}$ (i.e. a cross section) gives

$$(i_\omega)_E = i_\omega \int_0^\infty Q_{i\omega}(\tau) \int_{\mathscr{F}} v\overline{P_\omega}(\mathbf{x}_E, \mathbf{x}_\omega, \tau)\,\mathrm{d}E\,\mathrm{d}\tau, \tag{19}$$

if molecular and turbulent diffusion of species i across $\mathscr{F}$ in the longitudinal direction is negligible in comparison to the convective transport of species i across $\mathscr{F}$ in longitudinal direction. $\mathrm{d}E$ is an element of area of $\mathscr{F}$.

Let us consider the case that the formation of NO in the elements of burnt fluid from ω is frozen as they move through the outer zone towards the primary zone exit. The effect of this inhibition on the velocity field will be negligible. Hence, in the frozen case under consideration equation (19) takes the form, if i refers to NO,

$$1 = \int_0^\infty \int_{\mathscr{F}} v\overline{P_\omega}(\mathbf{x}_E, \mathbf{x}_\omega, \tau)\,\mathrm{d}E\,\mathrm{d}\tau. \tag{20}$$

The integral

$$\int_{\mathscr{F}} v\overline{P_\omega}(\mathbf{x}_E, \mathbf{x}_\omega, \tau)\,\mathrm{d}E$$

multiplied by a sufficiently small time interval describes the probability of finding the marked element of burnt fluid, which was at $\mathbf{x}_\omega$ at time $t-\tau$, in a thin disk at $\mathscr{F}$ at time t. Also, this integral can be expected to attain a sharp maximum at, say, $\tau = \tau_{\max}$ so that equation (19) can be written as

$$(i_\omega)_E = i_\omega Q_{i\omega}(\tau_{\max}) \tag{21}$$

to a good approximation. For $Q_{i\omega}(\tau_{\max})$ we obtain, using equations (13), (14) and the foregoing modelling concept,

$$Q_{i\omega}(\tau_{\max}) = \frac{c_{ie}(p_E, T_E, \Phi, \varepsilon, \Psi)}{c_i(\Phi, \varepsilon, \Psi)}. \tag{22}$$

The numerator denotes the equilibrium mass fraction of pollutant i in the elements of burnt fluid from ω when passing across the primary zone exit. The denominator denotes the mass fraction of pollutant i in the elements of burnt fluid under consideration when passing across ω. i_ω can be expressed as follows using equation (4) for N_2 and assumption (13) for N_2 and pollutant i

$$i_\omega = \frac{c_i(\Phi, \varepsilon, \Psi)}{c_{N_2}(\Phi, \varepsilon, \Psi)} g \frac{B}{\Omega} \tag{23}$$

where $c_{N_2}(\phi, \varepsilon, \Psi)$ denotes the mass fraction of N_2 in the elements of burnt fluid under consideration when passing across ω. Substituting equations (22) and (23) into equation (21) gives

$$(i_\omega)_E = \frac{c_{ie}(p_E, T_E, \Phi, \varepsilon, \Psi)}{c_{N_2}(\Phi, \varepsilon, \Psi)} g \frac{B}{\Omega}. \tag{24}$$

The ensemble-averaged outflow of pollutant i across the primary zone exit, e_i (i.e. the emission rate of pollutant i from the primary zone exit) is equal to the sum of all $(i_\omega)_E$

$$e_i = \sum_{\omega=1}^{\Omega} (i_\omega)_E. \tag{25}$$

The values of the ratios Φ, ε, Ψ in the various terms $(i_\omega)_E$ can be considered as the values taken on at the same time on the corresponding elements ω of $\mathscr{P}$. Note that $Q_{i\omega}$ does not depend on t and t_b separately but on the combination $t - t_b$ only.

If we consider Ω to be very large, equation (25) can then be rewritten in a good approximation to give

$$e_i = gB \int_{\Phi=0}^\infty \int_{\varepsilon=0}^\infty \int_{\Psi=0}^\infty \times \frac{c_{ie}(p_E, T_E, \Phi, \varepsilon, \Psi)}{c_{N_2}(\Phi, \varepsilon, \Psi)} w(\Phi, \varepsilon, \Psi)\,\mathrm{d}\Phi\,\mathrm{d}\varepsilon\,\mathrm{d}\Psi \tag{26}$$

where

$$\int_{\mathscr{L}} w(\Phi, \varepsilon, \Psi)\,\mathrm{d}\Phi\,\mathrm{d}\varepsilon\,\mathrm{d}\Psi$$

is the probability that Φ, ε, Ψ of an element ω of $\mathscr{P}$ chosen at random (trial of an experiment) lies in the region $\mathscr{L}$ of the Φ, ε, Ψ-space (sample space), all trials being carried through on the prototype at the same time.

Second 'closure assumption'

The density $w(\Phi, \varepsilon, \Psi)$ is a narrow, high spike attaining a sharp maximum at

$$\Phi = \hat{\Phi}, \quad \varepsilon = \hat{\varepsilon}, \quad \Psi = \hat{\Psi} \tag{27}$$

so that the integral on the RHS of equation (26) can be written as approximately

$$\int_{\Phi=0}^\infty \int_{\varepsilon=0}^\infty \int_{\Psi=0}^\infty \frac{c_{ie}(p_E, T_E, \Phi, \varepsilon, \Psi)}{c_{N_2}(\Phi, \varepsilon, \Psi)} \times w(\Phi, \varepsilon, \Psi)\,\mathrm{d}\Phi\,\mathrm{d}\varepsilon\,\mathrm{d}\Psi = \frac{c_{ie}(p_E, T_E, \hat{\Phi}, \hat{\varepsilon}, \hat{\Psi})}{c_{N_2}(\hat{\Phi}, \hat{\varepsilon}, \hat{\Psi})}. \tag{28}$$

$\hat{\Phi}, \hat{\varepsilon}$ and $\hat{\Psi}$ are the overall primary zone fuel to O_2 ratio, the N_2 to O_2 ratio and the water vapour to O_2 ratio of the air at the primary zone inlet, respectively.

By definition

$$\hat{\Phi} = \frac{F}{\gamma B} \tag{29}$$

where F is the ensemble-averaged fuel injection rate into the primary zone. γ denotes the O_2 to air ratio of the air at the primary zone inlet.

Determination of p_E and T_E

The determination of p_E and T_E is based on a 1-dim. flow model at the primary zone exit. Turbulence and molecular transport in the primary zone are built into this model through the pressure and the total pressure at the primary zone exit. These pressures are to be interpreted as time averages, averaged over the cross section, which are determined experimentally. The conservation of mass in the primary zone and the equation of state at the primary zone exit can then be written

$$\rho v E = A + F \tag{30}$$

and

$$p = \frac{R}{W}\rho T \tag{31}$$

where $p_E = p$, $T_E = T$ by definition and v, E, R and W denote, respectively, the flow velocity, the area of $\mathscr{F}$, the universal gas constant and the molecular weight of the gas. The gas mixture at the primary zone exit can be approximately treated as an ideal gas of molecular weight W and constant specific heat at constant pressure, c_p, in a steady inviscid equilibrium flow towards a reservoir indicated by the subscript t. This is because the Mach number

$$M = \frac{v}{a}$$

where

$$a^2 = \kappa\frac{R}{W}T,$$

$$\kappa = \frac{c_p}{c_p - \dfrac{R}{W}} \tag{32}$$

can be considered to be much smaller than one in the equilibrium flow towards the reservoir. The following relations hold for the flow towards the reservoir:

$$\frac{T_E}{T_t} = \frac{1}{1+\dfrac{\kappa-1}{2}M^2},$$

$$\frac{p_E}{p_t} = \left(1+\frac{\kappa-1}{2}M^2\right)^{-\kappa/(\kappa-1)}. \tag{33}$$

The following relationship between M and p_t, T_t will be employed:

$$\frac{A+F}{Ep_t}\left\{\frac{T_tR[c_p-(R/W)]}{Wc_p}\right\}^{1/2} = M\left(1+\frac{\kappa-1}{2}M^2\right)^{-(\kappa+1)/[2(\kappa-1)]} = M+O[M^3]. \tag{34}$$

W and c_p are expressed in terms of p_t and T_t as follows:

$$\frac{1}{W} = \sum_{j=1}^{n}\frac{c_j(T_t,p_t)}{W_j} \tag{35}$$

where W_j is the molecular weight of species j, and $c_j(T,p)$ denotes the equilibrium mass fraction of j.

$$c_p = \frac{\partial}{\partial T}\sum_{j=1}^{n} c_j(T,p)h_j(T) \tag{36}$$

where $h_j(T)$ is the enthalpy of species j per unit mass of j. The partial derivative on the RHS of equation (36) has to be evaluated at $T = T_t$, $p = p_t$. If the influence of dissociation on W and c_p is negligible we have

$$\frac{1}{W} = \sum_{j=1}^{5}\frac{(c_j)_0}{W_j}, \quad c_p = \sum_{j=1}^{5}(c_j)_0 c_{pj}(T_t). \tag{37}$$

$c_{pj}(T)$ denotes the specific heat at constant pressure of species j. $(\,)_0$ pertains to the composition at low temperatures where dissociation is negligible. The values $(c_j)_0$ are determined by means of equations (44)–(46). The species involved in relation (37) are compiled in Table 1. The subsequent calculation of c_p and W and T_t concerns the case in which the influence of dissociation on W and c_p is not negligible. The species and chemical reactions taken into account are compiled in Tables 1 and 2, respectively. Computations assuming that the NO concentration is controlled by the reaction $N_2+O_2 \leftrightarrows 2NO$ should be discounted because it is now believed that this reaction does not proceed directly (ref. [2], p. 843).

The reactions of Table 2 are independent. Hence, five linear relations of type (7) exist. These are

$$c_1 = (c_1)_0, \quad c_2 = (c_2)_0 \tag{38}$$

and the three equations expressing the conservation of oxygen, hydrogen and carbon atoms:

$$\frac{1}{2W_7}c_7 + \frac{1}{W_8}c_8 + \frac{1}{W_4}c_4 = \frac{1}{W_4}(c_4)_0, \tag{39}$$

$$\frac{1}{W_5}c_5 + \frac{1}{2W_6}c_6 + \frac{1}{2W_4}c_4 + \frac{1}{W_3}c_3 + \frac{1}{2W_7}c_7 = \frac{1}{W_5}(c_5)_0 + \frac{1}{2W_4}(c_4)_0 + \frac{1}{W_3}(c_3)_0, \tag{40}$$

$$\frac{1}{W_6}c_6 + \frac{1}{W_5}c_5 = \frac{1}{W_5}(c_5)_0. \tag{41}$$

The mass fractions $(c_j)_0, j = 1,\ldots,5$ can be expressed in terms of $F/(\gamma_d A)$, $\hat{\varepsilon}$, the Ar/N_2 ratio of the dry air at the primary zone inlet, χ, the H_2O-vapour to dry air ratio of the air at the primary zone exit, ψ, the mean equivalence ratio at the primary zone exit,

$$\varphi = \frac{F}{\gamma_d A}\frac{\nu_3' W_3}{\nu_f' W_f}(1+\psi), \tag{42}$$

and $(W_4\nu_4'')/(\nu_5'' W_5)$ where ν_f', ν_3', ν_4'', ν_5'' are the stoichiometric coefficients of the overall combustion process

$$\nu_f' f + \nu_3' O_2 \rightarrow \nu_4'' H_2O + \nu_5'' CO_2. \tag{43}$$

Table 1. Species of the fuel-lean exhaust gas at the primary zone exit

j	1	2	3	4	5	6	7	8
	N_2	Ar	O_2	H_2O	CO_2	CO	OH	H_2

Table 2. Model reaction scheme for gaseous dissociation and recombination reactions at the primary zone exit in the temperature range 2000–3000 K, pressure range 5–30 atm (ref. [13], p. 317)

$2CO+O_2 \leftrightarrows 2CO_2$	(1)
$2H_2+O_2 \leftrightarrows 2H_2O$	(2)
$H_2+2OH \leftrightarrows 2H_2O$	(3)

f stands for a fuel molecule, γ_d is the O_2 to air ratio of the dry air at the primary zone inlet, and W_f is the molecular weight of the fuel. A simple calculation gives

$$(c_1)_0 = \hat{\varepsilon} c_{O_2}, \quad (c_2)_0 = \hat{\varepsilon}\chi c_{O_2}, \quad (c_3)_0 = (1-\varphi)c_{O_2}, \tag{44}$$

$$(c_4)_0 = \left\{\psi[1+\hat{\varepsilon}(1+\chi)]c_{O_2} + \frac{\nu_4'' W_4}{\nu_5'' W_5}\right\}(c_5)_0, \tag{45}$$

$$(c_5)_0 = \frac{1-[1+\hat{\varepsilon}(1+\chi)-\varphi]c_{O_2}}{1+[(\nu_4'' W_4)/\nu_5'' W_5]+\psi[1+\hat{\varepsilon}(1+\chi)]c_{O_2}} \tag{46}$$

where, for brevity,

$$c_{O_2} = \frac{1}{[\{[F/(\gamma_d A)]+[1+\hat{\varepsilon}(1+\chi)]\}(1+\psi)]}. \tag{47}$$

Equations (38)-(41) are supplemented by the laws of mass action associated with the chemical reactions of Table 2

$$\frac{c_6^2 c_3}{c_5^2} = \frac{W_6^2 W_3 K_1(T_t)}{W_5^2 \rho_t}, \quad \frac{c_8^2 c_3}{c_4^4} = \frac{W_8^2 W_3 K_2(T_t)}{W_4^2 \rho_t}, \quad \frac{c_8 c_7^2}{c_4^2} = \frac{W_8 W_7^2 K_3(T_t)}{W_4^2 \rho_t} \tag{48}$$

where $K_r(T)$ is the equilibrium constant of the rth reaction of Tables 2 and 4. The calculation of $K_r(T)$ starts with equation (76). The solution $c_i, i = 1,\ldots,8$ of the system of equations (38)-(41) and (48) in terms of $(c_i)_0$, $i = 1,\ldots,5$; ρ_t and $K_r(T_t)$, $r = 1,2,3$ is found by trial and error. From this system it follows that the components $c_i, i \neq 1,2,5$ of the solution vector can be expressed in terms of $c_5, (c_i)_0 (i = 3,\ldots,5), \rho_t$ and $K_r(T_t)$ $(r = 1,2,3)$ as follows:

$$c_6 = \frac{W_6}{W_5}[(c_5)_0 - c_5], \tag{49}$$

$$c_3 = \frac{c_5^2 W_3 K_1(T_t)}{\rho_t[(c_5)_0 - c_5]^2},$$

$$c_7 = \frac{1}{2}\left\{-\left[\frac{W_7 K_3(T_t) c_3^{1/2}}{W_3^{1/2}\rho_t^{1/2} K_2(T_t)^{1/2}}\right] + W_7\left[\frac{K_3(T_t)c_3^{1/2}}{W_3^{1/2}\rho_t^{1/2}K_2(T_t)^{1/2}}\right]^{1/2} \times\left[\frac{K_3(T_t)c_3^{1/2}}{W_3^{1/2}\rho_t^{1/2}K_2(T_t)^{1/2}} + 4\beta\right]^{1/2}\right\} \tag{50}$$

where

$$\beta = \frac{(c_4)_0}{W_4} + \frac{1}{W_5}[(c_5)_0 - c_5] + \frac{2}{W_3}[(c_3)_0 - c_3], \tag{51}$$

$$c_4 = (c_4)_0 + \frac{W_4}{W_5}[(c_5)_0 - c_5] + \frac{2W_4}{W_3}[(c_3)_0 - c_3] - \frac{W_4}{W_7}c_7, \tag{52}$$

$$c_8 = \frac{W_8}{W_4}[(c_4)_0 - c_4] - \frac{W_8}{2W_7}c_7. \tag{53}$$

Equations (49)-(53) are supplemented by equation (38). The calculation of the components $c_i, i \neq 1, 2$, of the solution vector proceeds as follows: in the first step T_t and ρ_t are fixed estimates. The solution (49)-(53) for an estimated c_5 is checked against the compatibility relations $c_i \geqslant 0 (i = 1,\ldots,8)$ and equation (48) for $r = 2$ and 3, which are satisfied if the choice of c_5 was correct. In the second step ρ_t becomes a variable estimate. The correct solution associated with the estimates ρ_t and T_t is checked against the 'compatibility relation' $p_t = (\rho_t R T_t)/W$ where p_t is given and W is formed using the correct solution associated with the estimates ρ_t and T_t. If the latter compatibility relation is satisfied the correct solution associated with the estimates ρ_t and T_t is then checked (in a third step) against the 'compatibility relation' (33) for the pressure ratio. The LHS of this compatibility relation is given. The evaluation of its RHS relies on the estimated reservoir temperature T_t and employs equation (34). If the compatibility relation (33) is satisfied the equilibrium mass fractions inserted into this relation constitute the solution sought, and the estimate for T_t proves to be the reservoir temperature sought. Otherwise, the described procedure must be repeated using an improved estimate for T_t. The calculation of c_p involves partial derivatives of equilibrium mass fractions with respect to temperature at constant pressure. These derivatives are expressed in terms of the corresponding equilibrium mass fractions (at $p = p_t$, $T = T_t$) as follows:

$$\frac{\partial c_1}{\partial T} = \frac{\partial c_2}{\partial T} = 0, \tag{54}$$

$$\frac{1}{W_4}\frac{\partial c_4}{\partial T} + \frac{1}{2W_7}\frac{\partial c_7}{\partial T} + \frac{1}{W_8}\frac{\partial c_8}{\partial T} = 0, \tag{55}$$

$$\frac{1}{W_5}\frac{\partial c_5}{\partial T} + \frac{1}{W_6}\frac{\partial c_6}{\partial T} = 0, \tag{56}$$

$$\frac{1}{W_3}\frac{\partial c_3}{\partial T} + \frac{1}{2W_4}\frac{\partial c_4}{\partial T} + \frac{1}{W_5}\frac{\partial c_5}{\partial T} + \frac{1}{2W_6}\frac{\partial c_6}{\partial T} + \frac{1}{2W_7}\frac{\partial c_7}{\partial T} = 0, \tag{57}$$

$$-\frac{2}{c_4}\frac{\partial c_4}{\partial T} + \frac{2}{c_5}\frac{\partial c_5}{\partial T} - \frac{2}{c_6}\frac{\partial c_6}{\partial T} + \frac{2}{c_8}\frac{\partial c_8}{\partial T} = \frac{\Delta\hat{H}_2(T_t)}{\hat{R}T_t^2} - \frac{\Delta\hat{H}_1(T_t)}{\hat{R}T_t^2}, \tag{58}$$

$$-\frac{1}{c_3}\frac{\partial c_3}{\partial T} - \frac{2}{c_4}\frac{\partial c_4}{\partial T} + \frac{2}{c_5}\frac{\partial c_5}{\partial T} - \frac{2}{c_6}\frac{\partial c_6}{\partial T} + \frac{2}{c_7}\frac{\partial c_7}{\partial T} + \frac{1}{c_8}\frac{\partial c_8}{\partial T} = \frac{\Delta\hat{H}_3(T_t)}{\hat{R}T_t^2} - \frac{\Delta\hat{H}_1(T_t)}{\hat{R}T_t^2}, \tag{59}$$

$$\left(\frac{1}{c_3} - \frac{W}{W_3}\right)\frac{\partial c_3}{\partial T} - \frac{W}{W_4}\frac{\partial c_4}{\partial T} - \frac{2}{c_5}\frac{\partial c_5}{\partial T} + \frac{2}{c_6}\frac{\partial c_6}{\partial T} - \frac{W}{W_7}\frac{\partial c_7}{\partial T} - \frac{W}{W_8}\frac{\partial c_8}{\partial T} = \frac{\Delta\hat{H}_1(T_t)}{\hat{R}T_t^2}. \tag{60}$$

The derivatives in the system of equations (54)-(60)

must be evaluated under reservoir conditions. The RHS of equations (58)-(60) have been obtained utilizing van't Hoff's equations

$$\frac{\mathrm{d}\ln K_{pr}}{\mathrm{d}T} = \frac{\Delta\hat{H}_r}{\hat{R}T^2}, \quad r = 1,2,3 \tag{61}$$

where

$$K_{pr} = K_r(T)\frac{RT}{p^+}, \tag{62}$$

and

$$\Delta\hat{H}_r = \sum_{i=3}^{8}(v''_{ir} - v'_{ir})\hat{h}_i(T) \tag{63}$$

is the heat of reaction of the rth dissociation reaction. $\hat{R}$ denotes the universal gas constant per mole and p^+ is a reference pressure ($p^+ = 1$ atm in the numerical calculations). The enthalpy of species i per mole of i, $\hat{h}_i(T)$, can be written in the form

$$\hat{h}_i(T) = \hat{h}_i^{(0)} + \int_{T_0}^{T}\hat{c}_{pi}(T)\,\mathrm{d}T, \quad i = 1,\ldots,8 \tag{64}$$

where $\hat{c}_{pi}$ and $\hat{h}_i^{(0)}$ are, respectively, the specific heat of species i per mole of i at constant pressure and the enthalpy of formation of species i per mole of i at temperature T_0 ($T_0 = 298.15$ K in the numerical calculations). The superscript (0) denotes the standard state condition of 1 atm.

Statistical mechanics gives (ref. [15], p. 136)

$$\hat{c}_{pi}(T) = \hat{R}\left\{\frac{7}{2} + \left[\frac{\Theta_i/(2T)}{\sin h(\Theta_i/(2T))}\right]^2\right\} \tag{65}$$

for a pure diatomic gas i whose molecules behave as rigid rotators, simple harmonic vibrators, and exist only in their electronic ground state. Θ_i denotes the characteristic vibrational temperature of the diatomic species i. The corresponding formulae for gaseous CO_2 and gaseous H_2O are, respectively (ref. [16], pp. 74–76 and pp. 79–80)

$$\hat{c}_{p3}(T) = \hat{R}\left\{\frac{7}{2} + \sum_{v=1}^{4}\left[\frac{\Theta_{3v}/(2T)}{\sin h(\Theta_{3v}/(2T))}\right]^2\right\} \tag{66}$$

and

$$\hat{c}_{p4}(T) = \hat{R}\left\{4 + \sum_{v=1}^{3}\left[\frac{\Theta_{4v}/(2T)}{\sin h(\Theta_{4v}/(2T))}\right]^2\right\}. \tag{67}$$

Θ_{iv} denotes the characteristic vibrational temperature of the vth vibrational mode of the triatomic species i. It should be noted that CO_2 is a linear molecule, whilst H_2O is a nonlinear molecule, and linear triatomic molecules have one degenerate bending vibration. Statistical mechanics gives simply

$$\hat{c}_{pi}(T) = \tfrac{5}{2}\hat{R} \tag{68}$$

for a pure monatomic gas i whose atoms exist only in their electronic ground state.

Table 3. Characteristic vibrational temperatures [K] (ref. [14], p. 615 and chapter 63)

Θ_1	Θ_3	Θ_6	Θ_7	Θ_8	Θ_{11}
3352	2228	3080	4895	5995	2700.6
Θ_{41}	Θ_{42}	Θ_{43}	Θ_{51}	Θ_{52}	$\Theta_{53} = \Theta_{54}$
5258	5400	2293	1924	3379	961

Calculation of NO emission from the primary zone

The general formula, equations (26) and (28), gives

$$e_{11} = gB\frac{c_{11_e}(p_E, T_E, \hat{\Phi}, \hat{\varepsilon}, \hat{\Psi})}{c_{N_2}(\hat{\Phi}, \hat{\varepsilon}, \hat{\Psi})}. \tag{69}$$

The thermodynamic and the chemical model to be associated with the mass fractions c_{11_e} and c_{N_2} in formula (69)* agree with the thermodynamic and the chemical part, respectively, of the 1-dim. flow model at the primary zone exit in the absence of the NO formation reactions compiled in Table 4. However, the composition of the unburnt mixture underlying c_{11_e} and c_{N_2} in equation (69) differs from the corresponding composition employed in the 1-dim. flow model at the primary zone exit by the value of Φ. This can be seen from equations (29) and (42). The deviation in Φ is small. This is because $(A-B)/A$ can be considered to be small. The deviation of W in the equation of state (31) from the mean molecular weight associated with the elements of burnt fluid under consideration when passing across the primary zone exit can be neglected in the temperature range 2000–3000 K, pressure range 5–30 atm. This is evident from extensive numerical calculations.

For brevity, we denote by c_i the mass fraction of species i in an element of burnt fluid under consideration when passing across the primary zone exit. The laws of mass action associated with the reaction scheme of Table 4 give

$$c_9 = c_1^{1/2}\left[\frac{K_4(T_E)^{1/2}W_9}{\rho_E^{1/2}W_1^{1/2}}\right], \quad c_{10} = c_3^{1/2}\left[\frac{K_5(T_E)^{1/2}W_{10}}{\rho_E^{1/2}W_3^{1/2}}\right],$$

$$c_{11} = (c_1c_3)^{1/2}[K_6(T_E)K_7(T_E)]^{1/2}W_{11}(W_1W_3)^{-1/2}. \tag{70}$$

Conservation of mass in the model reaction scheme of Table 4 yields

$$c_1 + c_3 + c_9 + c_{10} + c_{11} = (c_1 + c_3)_f \tag{71}$$

where $(\,)_f$ pertains to the case of frozen NO formation reactions of Table 4 in the elements of burnt fluid under

Table 4. Model reaction scheme for NO formation. The reactions (6) and (7) constitute the Zeldovich mechanism

$N_2 \leftrightarrows 2N$	(4)
$O_2 \leftrightarrows 2O$	(5)
$O + N_2 \leftrightarrows N + NO$	(6)
$N + O_2 \leftrightarrows O + NO$	(7)

* i.e. the thermodynamic and the chemical model associated with elements of burnt fluid for which $\Phi = \hat{\Phi}$, $\Psi = \hat{\Psi}$, $\varepsilon = \hat{\varepsilon}$.

Table 5. Species involved in the model reaction scheme of Table 4

i	9	10	11	1	3
	N	O	NO	N_2	O_2

consideration. $(c_1)_f, (c_3)_f$ are the components c_1, c_3 of the solution of equations (38)-(41) and (48) for $\rho_t = \rho_E$, $T_t = T_E$, $\Phi = [F(1+\psi)]/(\gamma_d B)$. Dissociation of N_2 is small in the elements of burnt fluid under consideration so that we can substitute

$$c_1 = (c_1)_f = c_{N_2}(\hat{\Phi}, \hat{\varepsilon}, \hat{\Psi}) = \frac{\hat{\varepsilon}}{1+\hat{\varepsilon}+\chi\hat{\varepsilon}+\hat{\Phi}+(\psi/\gamma_d)} \quad (72)$$

in equations (70) and (71). From equations (70)–(72) it follows that

$$c_3^{1/2} = \tfrac{1}{2}[-P+(P^2-4Q)^{1/2}] \quad (73)$$

where

$$P = \frac{K_5(T_E)^{1/2}W_3^{1/2}}{2\rho_E^{1/2}} + \frac{(c_1)_f^{1/2}K_6(T_E)^{1/2}K_7(T_E)^{1/2}W_{11}}{(W_1W_3)^{1/2}}, \quad (74)$$

$$Q = \frac{(c_1)_f^{1/2}K_4(T_E)^{1/2}W_1^{1/2}}{(2\rho_E^{1/2})} - (c_3)_f. \quad (75)$$

The calculation of the equilibrium constants $K_r(T)$, $r = 1,\ldots,7$ starts with the integration of the van't Hoff equation. This first step gives

$$K_r(T) = K_{pr}(T_B)\left(\frac{p^+}{RT}\right)^{\alpha_r} e^{I_r(T)}, \quad r = 1,\ldots,7 \quad (76)$$

where

$$\left.\begin{aligned} &\alpha_r = 1 \quad \text{for} \quad r = 1,\ldots,5; \quad \alpha_6 = \alpha_7 = 0, \\ &I_r(T) = \int_{T_B}^{T} \frac{\Delta\hat{H}_r(\vartheta)}{\hat{R}\vartheta^2}\,\mathrm{d}\vartheta. \end{aligned}\right\} \quad (77)$$

ϑ is an integration variable. T_B denotes a reference temperature ($T_B = 2500$ K in the numerical calculations, the values $K_{pr}(T_B)$, $r = 1,\ldots,7$ are taken from chapter 343 in ref. [14]). The integrals $I_r(T)$ can be calculated analytically to give:

$$I_1(T) = E_{3t}(T)+E_3(T)-2\left[E_{5t}(T)+E_5(T)+\frac{\hat{h}_5^{(0)}}{\hat{R}}\left(\frac{1}{T_B}-\frac{1}{T}\right)\right]+2\left[E_{6t}(T)+E_6(T)+\frac{\hat{h}_6^{(0)}}{\hat{R}}\left(\frac{1}{T_B}-\frac{1}{T}\right)\right], \quad (78)$$

$$I_2(T) = E_{3t}(T)+E_3(T)-2\left[E_{4t}(T)+E_4(T)+\frac{\hat{h}_4^{(0)}}{\hat{R}}\left(\frac{1}{T_B}-\frac{1}{T}\right)\right]+2\left[E_{8t}(T)+E_8(T)+\frac{\hat{h}_8^{(0)}}{\hat{R}}\left(\frac{1}{T_B}-\frac{1}{T}\right)\right], \quad (79)$$

$$I_3(T) = -2\left[E_{4t}(T)+E_4(T)+\frac{\hat{h}_4^{(0)}}{\hat{R}}\left(\frac{1}{T_B}-\frac{1}{T}\right)\right]+2\left[E_{7t}(T)+E_7(T)+\frac{\hat{h}_7^{(0)}}{\hat{R}}\left(\frac{1}{T_B}-\frac{1}{T}\right)\right]+E_{8t}(T)+E_8(T)+\frac{\hat{h}_8^{(0)}}{\hat{R}}\left(\frac{1}{T_B}-\frac{1}{T}\right), \quad (80)$$

$$I_4(T) = -E_{1t}(T)+2E_9(T)-E_1(T)+\frac{2\hat{h}_9^{(0)}}{\hat{R}}\left(\frac{1}{T_B}-\frac{1}{T}\right), \quad (81)$$

$$I_5(T) = -E_{3t}(T)+2E_{10}(T)-E_3(T)+\frac{2\hat{h}_{10}^{(0)}}{\hat{R}}\left(\frac{1}{T_B}-\frac{1}{T}\right), \quad (82)$$

$$I_6(T) = -E_{1t}(T)+E_{11t}(T)+\frac{\hat{h}_9^{(0)}-\hat{h}_{10}^{(0)}+\hat{h}_{11}^{(0)}}{\hat{R}}\left(\frac{1}{T_B}-\frac{1}{T}\right), \quad (83)$$

$$I_7(T) = -E_{3t}(T)+E_{11t}(T)+\frac{\hat{h}_{10}^{(0)}+\hat{h}_{11}^{(0)}-\hat{h}_9^{(0)}}{\hat{R}}\left(\frac{1}{T_B}-\frac{1}{T}\right). \quad (84)$$

The functions $E_{it}(T)$ and $E_i(T)$ are defined by

$$E_{it}(T) = \ln\left(\frac{e^{\Theta_i/T_B}-1}{e^{\Theta_i/T}-1}\right)+\left(\frac{1}{e^{\Theta_i/T_0}-1}+1\right)\left(\frac{\Theta_i}{T}-\frac{\Theta_i}{T_B}\right), \quad i = 1,3,6,7,8,11, \quad (85)$$

$$E_{4t}(T) = \sum_{\nu=1}^{3}\ln\frac{e^{\Theta_{4\nu}/T_B}-1}{e^{\Theta_{4\nu}/T}-1}+\sum_{\nu=1}^{3}\Theta_{4\nu}\times\left(1+\frac{1}{e^{\Theta_{4\nu}/T_0}-1}\right)\left(\frac{1}{T}-\frac{1}{T_B}\right), \quad (86)$$

$$E_{5t}(T) = \sum_{\nu=1}^{4}\ln\frac{e^{\Theta_{5\nu}/T_B}-1}{e^{\Theta_{5\nu}/T}-1}+\sum_{\nu=1}^{4}\Theta_{5\nu}\times\left(1+\frac{1}{e^{\Theta_{5\nu}/T_0}-1}\right)\left(\frac{1}{T}-\frac{1}{T_B}\right), \quad (87)$$

$$\frac{E_i(T)}{\ln(T/T_B)+(T_0/T)-(T_0/T_B)} = \begin{cases} \frac{5}{2} \text{ for } i = 9,10, \\ \frac{7}{2} \text{ for } i = 1,3,5,6,7,8, \\ 4 \text{ for } i = 4. \end{cases} \quad (88)$$

The enthalpies of formation appearing in the analytical expressions for $K_r(T)$ are taken from Table 1 in ref. [17]. Equations (70), (72), (73)–(75) and (29) lead to

$$\frac{c_{11e}(p_E, T_E, \hat{\Phi}, \hat{\varepsilon}, \hat{\Psi})}{c_{N_2}(\hat{\Phi}, \hat{\varepsilon}, \hat{\Psi})} = \frac{W_{11}[K_6(T_E)K_7(T_E)]^{1/2}}{2(W_1W_3)^{1/2}(c_1)_f^{1/2}} \times[-P+(P^2-4Q)^{1/2}] \quad (89)$$

where

$$(c_1)_f = \frac{\hat{\varepsilon}}{1+\hat{\varepsilon}+\chi\hat{\varepsilon}+[F(1+\psi)/(\gamma_d B)]+(\psi/\gamma_d)}, \quad \hat{\Phi} = \frac{F(1+\psi)}{\gamma_d B}, \quad \frac{\psi}{\gamma_d} = \hat{\Psi}, \quad (90)$$

$$P=\frac{W_3^{1/2}K_5(T_E)^{1/2}}{2\rho_E^{1/2}}+\frac{[K_6(T_E)K_7(T_E)]^{1/2}W_{11}(c_1)_f^{1/2}}{(W_1W_3)^{1/2}}, \quad (91)$$

$$Q=\frac{(c_1)_f^{1/2}K_4(T_E)^{1/2}W_1^{1/2}}{2\rho_E^{1/2}}-(c_3)_f. \quad (92)$$

The equilibrium constants $K_r(T)$, $r=4,5,6,7$ are specified as functions of T by equations (76), (77), (81)–(85) and (88). $(c_3)_f$ is specified (for a given fuel of the form $C_lH_mO_n$) as a function of the variable quantities ρ_E, T_E, $\hat{\Phi}$ and ψ.

The result for the system function providing the NO emission from the primary zone exit in terms of engine-operating parameters relevant to the NO emission from the primary zone can now be expressed. Consider the model Mo whose gross structure is illustrated in Fig. 3. A, B, C denote, respectively, the fluid mechanical model underlying the general equations (26) and (28), the thermodynamic model underlying equation (89) (i.e. a mixture of thermally perfect gases) and the reaction scheme compiled in Tables 2 and 4. The model Mo provides e_{11}/B in terms of the variable quantities $T_E, \rho_E, F/B, \psi$ and $C_lH_mO_n$. The 1-dim. flow model at the primary zone exit, Mo1, specifies T_E and ρ_E as functions of the variable quantities $p_E, p_t, F/A, A/E, \psi$ and $C_lH_mO_n$. Hence, a connection in series of the two models as illustrated in Fig. 4 provides e_{11}/B in terms of the variable quantities p_E, p_t, F/A, B/A, A/E, ψ and $C_lH_mO_n$. Figure 4 is in accord with Fig. 3. Note that the thermodynamic and chemical part of Mo encompass the corresponding parts of Mo1 and the fluid mechanical model A in Fig. 3 can be considered to encompass both the fluid mechanical part of Mo and Mo1.

The concept of modelling as illustrated in Fig. 4 may be appropriate for the purpose of calculating the emission of other pollutants: soot, CO, hydrocarbons. Clearly, the thermodynamic and chemical part of Mo has to be replaced by appropriate submodels for this purpose. The present model whose gross structure is shown in Fig. 4 is appropriate, for instance, for aircraft gas turbine engine* operation at low altitude and

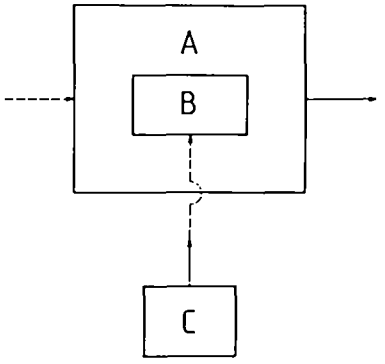

FIG. 3. Gross structure of the present model. A: Fluid mechanical model. B: Thermodynamic model. C: Chemical model.

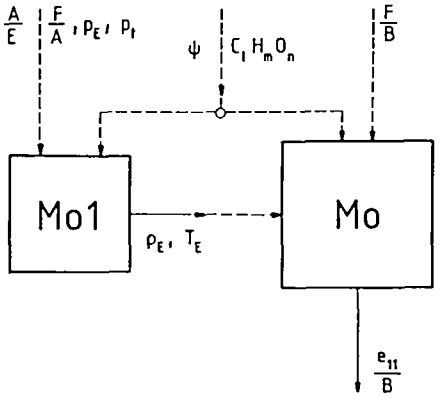

FIG. 4. Connection in series of the two models Mo and Mo1.

maximum thrust associated with the following conditions at the primary zone exit: pressure level 15–30 atm, temperature level 2500–3000 K, $(A/E) \geqslant 10$. The condition on the mass flow will be discussed in the next section. F, ψ and $C_lH_mO_n$ can be varied independently on a specific gas turbine engine. Under static thrust condition† p_E, p_t, A and B are particular functions of F, ψ and $C_lH_mO_n$, and the following relation holds:

$$\frac{J}{A-J}=\frac{\psi-\psi_z}{1+\psi_z} \quad (93)$$

where J and ψ_z are, respectively, the water injection rate and the water vapour/dry air ratio of the ambient air.

NUMERICAL RESULTS

Figure 5 illustrates the general system function of the mathematical model whose gross structure is shown in Fig. 4. Note that F/A can be expressed by equation (42) in terms of the mean equivalence ratio at the primary zone exit, φ, and ψ, at a given fuel of the form $C_lH_mO_n$. Figure 5 is based on the fuel C_2H_2 and is subdivided into three parts (1, 2, 3 from left to right) by the two lines $1-(p_E/p_t)=10^{-3}$ and 10^{-2}. The parameter values of the curves in part n ($n=1,2,3$) are listed within part n. All curves represented in Fig. 5 are practically straight lines and are associated with the same T_E-interval: 2700 K $\leqslant T_E \leqslant$ 3040 K. Results for T_E and e_{11}/B are marked as follows:

Part 1: (1) ——— T_E; (2) × ×; (3) ○———○ e_{11}/B; (4) ⊗ ⊗

Part 2: (5) – – – – – T_E; (6) △– – –△; (7) ⊙– – –⊙ e_{11}/B; (8) + +

* i.e. conventional single- (or twin-) spool axial flow turbo-jet engine with or without by-pass or front fan or aft fan; no afterburning.

† i.e. aircraft at rest in still air of given thermodynamic state at sea level.

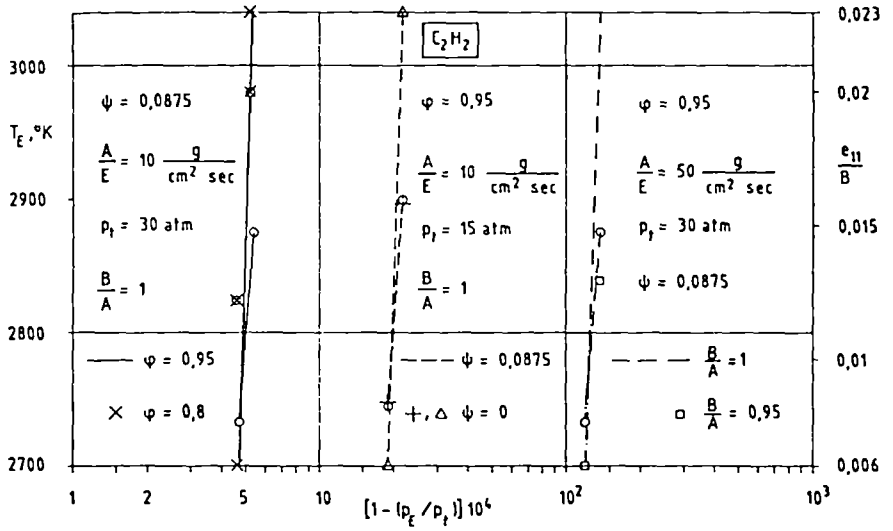

FIG. 5. Behaviour of the general system function of the combustor primary zone model.

Part 3: (9) —·—·—·—· T_E
(10) ⊙—·—·—·—⊙ } e_{11}/B.
(11) □ □ }

Curves (2), (4), (8) and (11) are plotted by two points each which are associated with the T_E-values 2700 K and 3040 K, respectively. $\psi = 0.0875$ is the ψ-value of saturated humid air at sea level, temperature 50°C and pressure 1000 mbar. Part 3 of Fig. 5 shows a significant effect of air flow distribution, described by B/A, on NO-emission from the primary zone.

It is readily seen from equations (33)-(36) and $M \ll 1$ that $(p_t - p_E)/p_t$ is proportional to A/E at fixed p_t, T_t, F/A, ψ and $C_lH_mO_n$. The choice of $(p_t - p_E)/p_t$ as an input quantity to be determined experimentally will be appropriate for sufficiently large A/E.

Figure 6 illustrates the effect of dissociation on the flow at the primary zone exit, after the model Mo1. All graphs in Fig. 6 are associated with the same T_E-interval: 2708 K $\leqslant T_E \leqslant$ 3050 K. $(\ )_f$ pertains to the case without dissociation (i.e. the reactions compiled in Table 2 are inhibited).

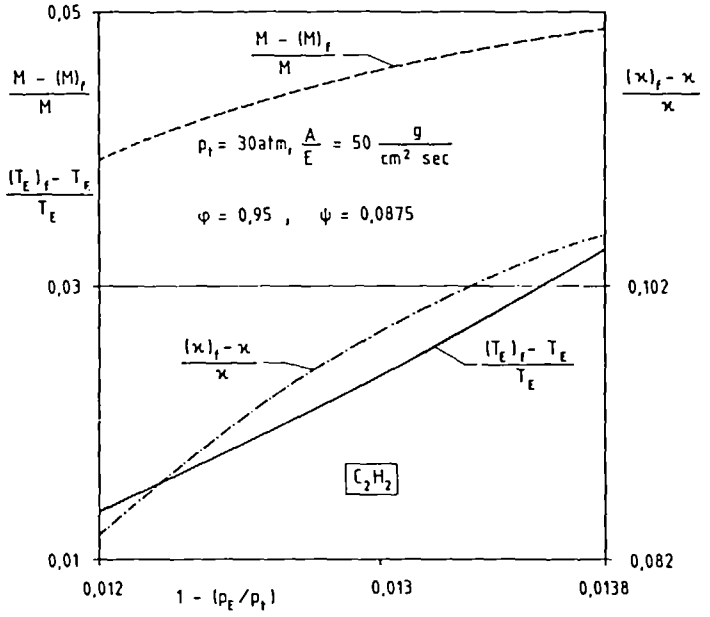

FIG. 6. Effect of dissociation on the flow at the primary zone exit.

REFERENCES

1. A. H. Lefebvre and R. S. Fletcher, AGARD-CP-125, p. 30 (1973).
2. J. B. Heywood, J. A. Fay and L. H. Linden, *AIAA J.* **9**, 841 (1971).
3. The jet engine, Rolls-Royce publications ref. T.S,D 1302 (2nd ed) (1966).
4. R. S. Fletcher and J. B. Heywood, AIAA Paper No. 71–123.
5. J. W. Sanborn, R. S. Reynolds and H. C. Mongia, AIAA Paper No. 76–682.
6. P. G. Felton *et al.*, AFOSR TR 77-1297, University Sheffield, Dept. of Chem. Eng. and Fuel Techn.
7. J. M. Beér and N. A. Chigier, *Combustion Aerodynamics*. Applied Science, London (1972).
8. K. N. C. Bray, Engineering applications of non-equilibrium flow theory, Cosserat Session, International Centre for Mechanical Sciences, Udine, Italy (1972).
9. P. A. Libby and F. A. Williams, *Ann. Rev. Fluid Mech.* **8**, 351 (1976).
10. M. Barrère, AGARD-CP-125 (1973).
11. R. F. Sawyer, Combustion rates in *Combustion-Generated Air Pollution* (edited by E. S. Starkman). Plenum Press, New York (1971).
12. J. B. Heywood and Th. Mikus, AGARD-CP-125 (1973).
13. E. Schmidt, *Technische Thermodynamik*, Bd. 2. Springer, Berlin (1977).
14. *D'Ans-Lax Taschenbuch für Chemiker und Physiker*, Band I. Springer, Berlin (1967).
15. W. G. Vincenti and Ch. H. Kruger, *Introduction to Physical Gas Dynamics*. Wiley, New York (1965).
16. E. A. Guggenheim, Thermodynamics, classical and statistical, in *Handbuch der Physik* (edited by S. Flügge) Vol. III/2. Springer, Berlin (1959).
17. L. S. Caretto and R. F. Sawyer, Combustion thermodynamics, in *Combustion-Generated Air Pollution* (edited by E. S. Starkman). Plenum Press, New York (1971).

MODELISATION D'UNE CHAMBRE DE COMBUSTION DE TURBINE A GAZ POUR LE CALCUL DES EMISSIONS DE POLLUANTS

Résumé—Deux aspects des écoulements de zone primaire dans les chambres de combustion—réservoir et annulaire—sont considérés en détail. D'abord, la production de polluants et le transport dans la zone primaire sont décrits par un modèle mathématique à trois dimensions. Ensuite, l'état mécanique et thermodynamique de l'écoulement à la sortie de l'écoulement primaire est décrit par un modèle mathématique á une dimension. La fonction générale d'une connexion en série de deux modèles fournit l'émission NO de la zone primaire en fonction des paramètres opératoires comme le débit d'injection de fuel et le débit d'injection d'eau. La méthode de modélisation montre un effet important du rapport entrée d'air de refroidissement/entrée d'air de combustion sur l'émission de NO. On analyse aussi l'influence de la dissociation sur l'écoulement à la sortie de la zone primaire.

MODELLIERUNG VON GASTURBINENBRENNKAMMERN ZUR BERECHNUNG DER SCHADSTOFFEMISSION

Zusammenfassung—Die Primärzonenströmung in Rohr- und Ringbrennkammern wird unter zwei Gesichtspunkten betrachtet. Schadstoffproduktion und Transport in der Primärzone werden durch ein dreidimensionales mathematisches Modell beschrieben. Der mechanische und thermodynamische Zustand der Strömung am Primärzonenausgang wird durch ein eindimensionales mathematisches Modell beschrieben. Die allgemeine Systemfunktion der Reihenschaltung aus den beiden Modellen liefert die NO-Emission aus der Primärzone in Abhängigkeit von Betriebsgrößen wie Brennstoffeinspritzrate und Wassereinspritzrate. Die Modellierung zeigt einen wesentlichen Einfluß des Verhältnisses Kühlluft- zu Verbrennungsluftdurchsatz auf die NO-Emission. Weiter wird Einfluß der Dissoziation auf die Strömung am Primärzonenaustritt gezeigt.

МОДЕЛИРОВАНИЕ КАМЕР СГОРАНИЯ ГАЗОВЫХ ТУРБИН ДЛЯ РАСЧЕТА КОЛИЧЕСТВА ЗАГРЯЗНЯЮЩЕГО ВЕЩЕСТВА

Аннотация—Подробно рассмотрены два аспекта течений в начальной зоне камер сгорания. Во-первых, образование и транспортировка загрязняющего вещества в начальной зоне описаны с помощью трехмерной математической модели. Во-вторых, механическое и термодинамическое состояние потока на выходе из начальной зоны описано с помощью одномерной математической модели. Функция состояния всей системы, полученная с помощью этих двух моделей, описывает эмиссию NO из начальной зоны с помощью таких рабочих параметров аппарата, как скорость ввода топлива и воды. Этот метод моделирования демонстрирует большое влияние на эмиссию NO отношения расхода охлаждающего воздуха к расходу воздуха, идущего на сжигание топлива. Анализируется также влияние диссоциации на поток на выходе из начальной зоны.